Angewandte Chemie
Eine Zeitschrift der Gesellschaft Deutscher Chemiker

Supporting Information

69451 Weinheim, Germany

Insights into the Catalytic Activity of Nitridated Fibrous Silica (KCC-1) Nanocatalysts from ^{15}N and ^{29}Si NMR Spectroscopy Enhanced by Dynamic Nuclear Polarization**

Aany Sofia Lilly Thankamony, Cédric Lion, Frédérique Pourpoint, Baljeet Singh, Angel J. Perez Linde, Diego Carnevale, Geoffrey Bodenhausen, Hervé Vezin, Olivier Lafon, and Vivek Polshettiwar**

anie_201406463_sm_miscellaneous_information.pdf

1. Chemicals and samples

1-1. Synthesis of bTbK

General procedures

All reagents and solvents were purchased from Sigma-Aldrich Chimie (Saint-Quentin-Fallavier, France) and used without further purification. Thin layer chromatography analyses were performed on aluminum sheets coated with silica gel 60F254 from Merck, while column chromatography purifications were carried out using Merck SiO_2 40-63 mesh. Proton and carbon nuclear magnetic resonance spectra were recorded on a Bruker AC300 spectrometer in deuterated chloroform. Chemical shifts δ are reported in part per million (ppm) downfield from TMS, and referenced with respect to the residual $CHCl_3$ signals (singlet at δ 7.26 ppm for ^1H NMR and central peak of $CDCl_3$ triplet at δ 77.16 ppm for ^{13}C NMR). Melting points were measured using a Thermo Scientific Electrothermal Melting Point 9100 apparatus and are reported uncorrected. Mass spectra were recorded on an Applied Biosystems Voyager DE-STR MALDI-TOF spectrometer, using dihydroxybenzoic acid as matrix.

Preparation of the bispiroketal diamine precursor

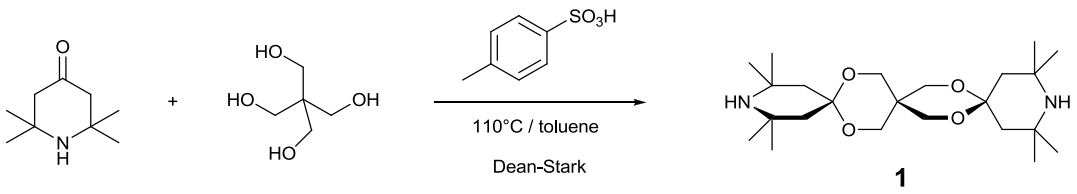

Scheme S1. Reaction scheme for the synthesis of bispiroketal diamine.

In a round-bottom flask equipped with a Dean-Stark trap, *para*-toluenesulfonic acid monohydrate (2.45 g, 12.9 mmol, 1.1 eq) was refluxed in toluene (50 mL) for 30 min for azeotropic removal of the water, and allowed to cool down. 2,2,6,6-tetramethylpiperidin-4-one (2.00 g, 12.88 mmol, 1 eq) and pentaerythritol (0.87 g, 6.4 mmol, 0.5 eq) were added, and the mixture was refluxed again until a white precipitate appeared. Dimethylformamide (5 mL) was then introduced dropwise and the reflux was maintained for 12 hours, at which point water accumulation in the Dean-Stark trap ceased. The reaction mixture was allowed to cool down and washed with 1.0 M aqueous sodium hydroxide (3 x 10 mL), water (2 x 10 mL) and brine (10 mL). The organic phase was then dried over sodium sulfate and the solvent was removed under reduced pressure. The resulting brown solid residue was recrystallized from a mixture of toluene and cyclohexane (v/v 1:1) to afford bispiroketaldiamine **1** as tan-colored

crystals (2.49 g, 6.05 mmol, 94%). Mp = 115-116°C. ^{1}H NMR (300 MHz, $CDCl_3$): δ 3.76 (s, 1H), 1.67 (s, 2H), 1.20 (s, 4H). ^{13}C NMR (75 MHz, $CDCl_3$): δ 99.60 (C^q), 63.48 (CH_2), 51.05 (CH_2), 43.02 (C^q), 32.52 (C^q), 32.19 (CH_3). IR (cm^{-1}): υ 3742, 1743, 1512, 1242, 1195, 1165, 1080. *m/z* = 411.3 $[M+H]^+$, 433.3 $[M+Na]^+$.

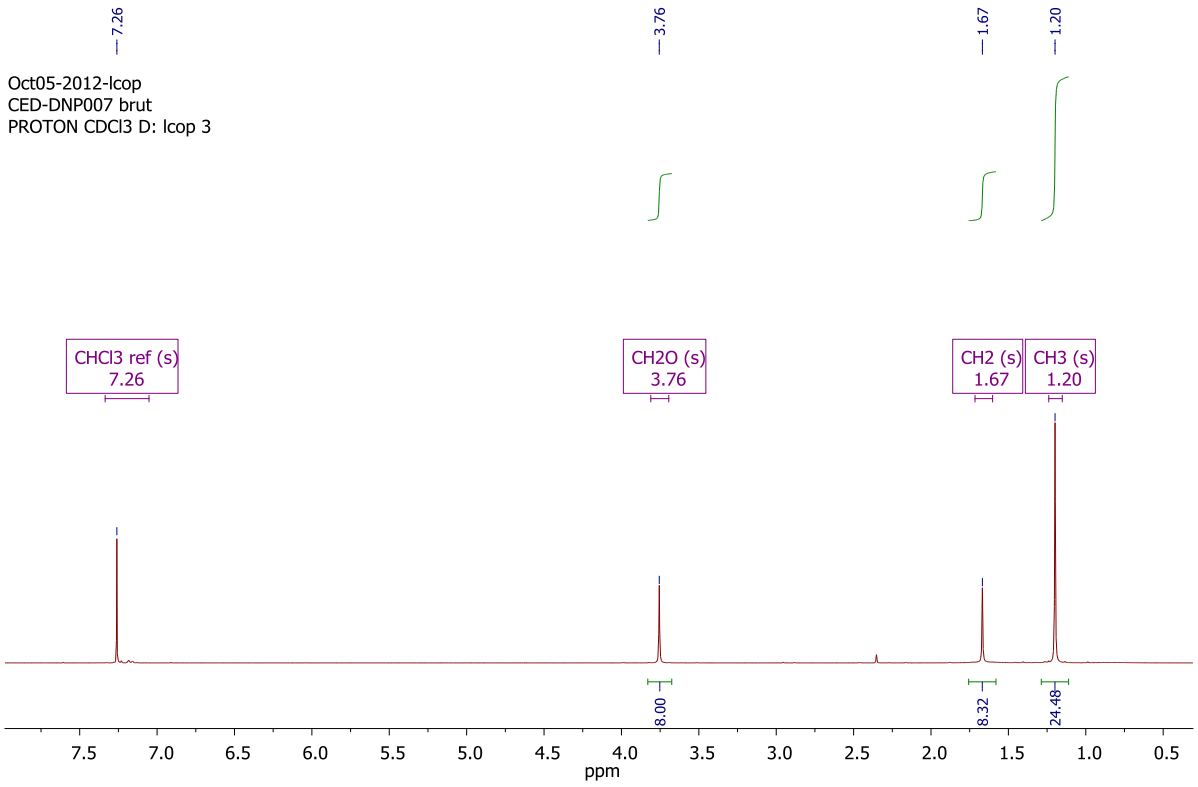

Figure S1. Diamine precursor **1** ^{1}H NMR spectrum ($CDCl_3$, 300 MHz.)

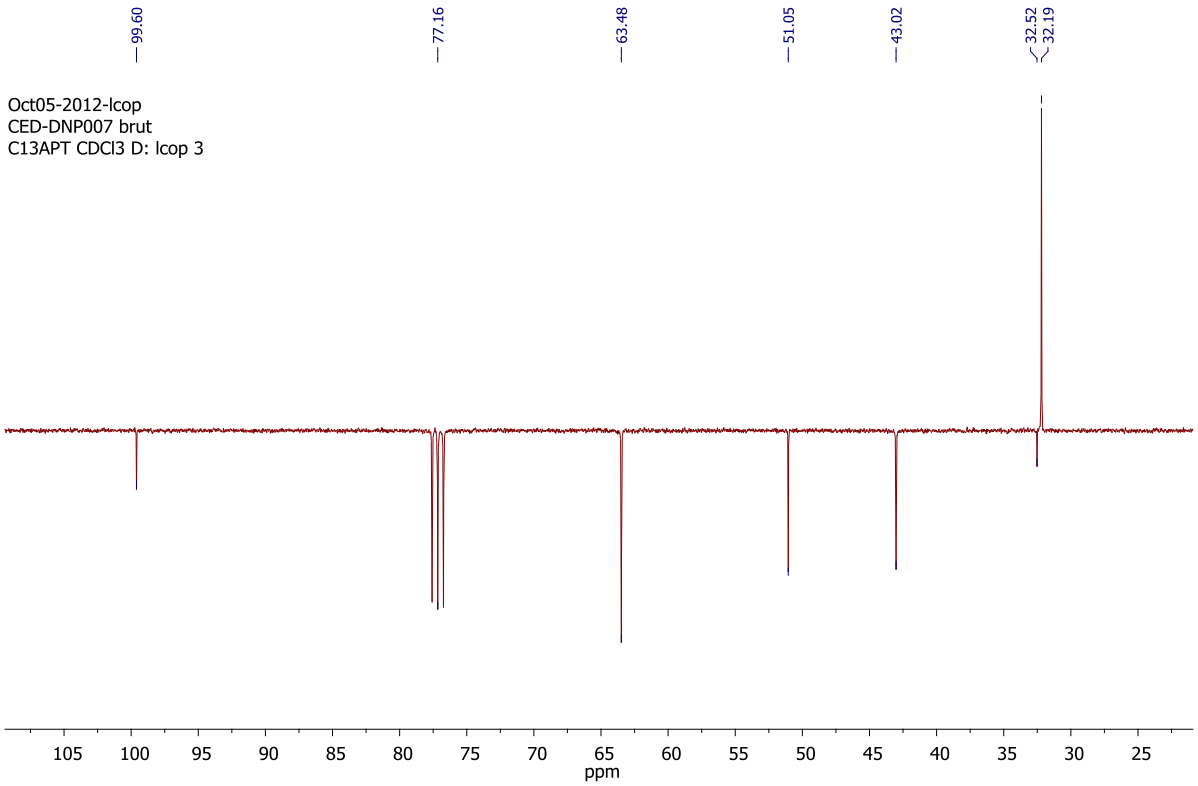

Figure S2. Diamine precursor **1** ^{13}C APT NMR spectrum ($CDCl_3$, 300 MHz.)

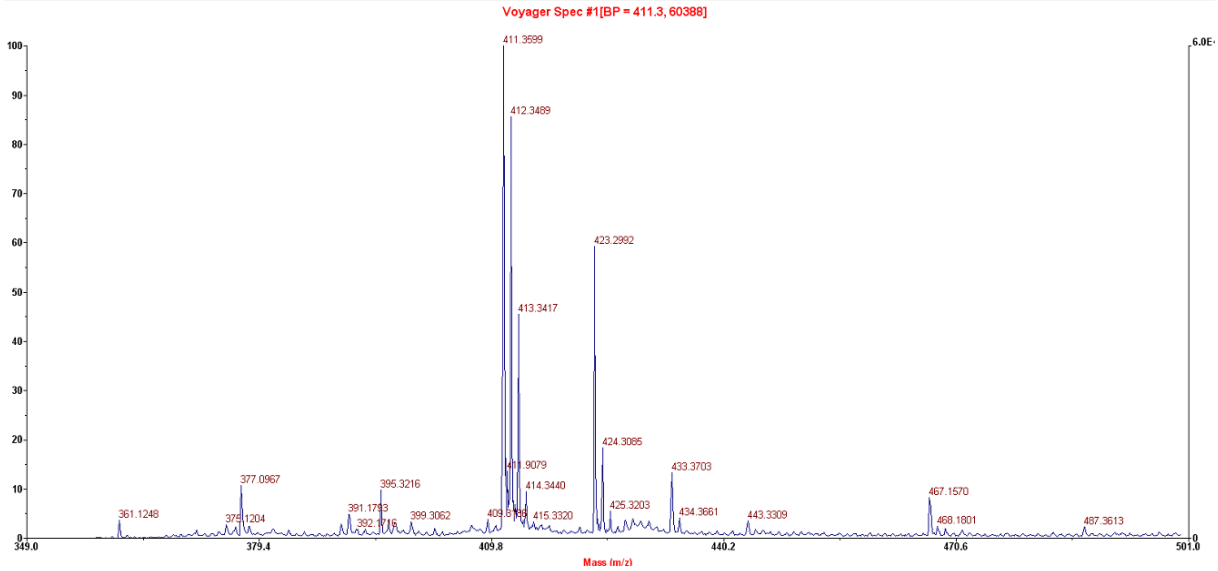

Figure S3. Diamine precursor **1** - MALDI-TOF mass spectrum (dihydroxybenzoic acid matrix.)

Preparation of dinitroxide bTbK

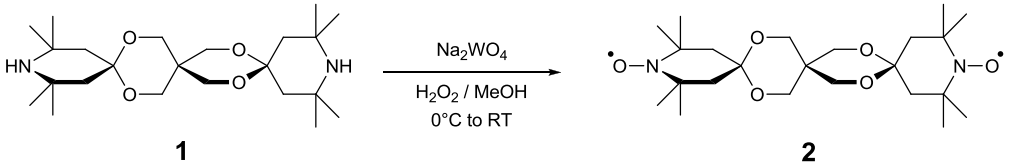

Scheme S2. Reaction scheme for the synthesis of bTbK.

Bispiroketaldiamine **1** (200 mg, 0.487 mmol, 1 eq) and sodium tungstate dihydrate (80 mg, 0.242 mmol, 0.5 eq) were dissolved in methanol (3 mL). The reaction mixture was cooled down to 0°C and a 30% v/v solution of hydrogen peroxide in water (1.0 mL, 9.8 mmol) was added dropwise over 15 minutes. It was then allowed to reach room temperature and stirred for 24 hours. The solution was saturated with potassium carbonate and extracted with chloroform (3 × 2 mL). The combined organic phases were dried over magnesium sulfate and the solvent was removed under reduced pressure. The residue was purified by flash chromatography ($CHCl_3$/MeOH 98:2) to afford bTbK as a red-orange solid (116 mg, 0.262 mmol, 54%). Mp = 166-167°C. IR (cm^{-1}): υ 1458, 1342, 1242, 1188, 1088, 1033. *m/z* = 425.2 $[MH\text{-}O]^+$, 441.3 $[MH]^+$, 442.2 $[MH_2]^{+\bullet}$, 443.2 $[MH_3]^+$, 463.3 $[M+Na]^+$.

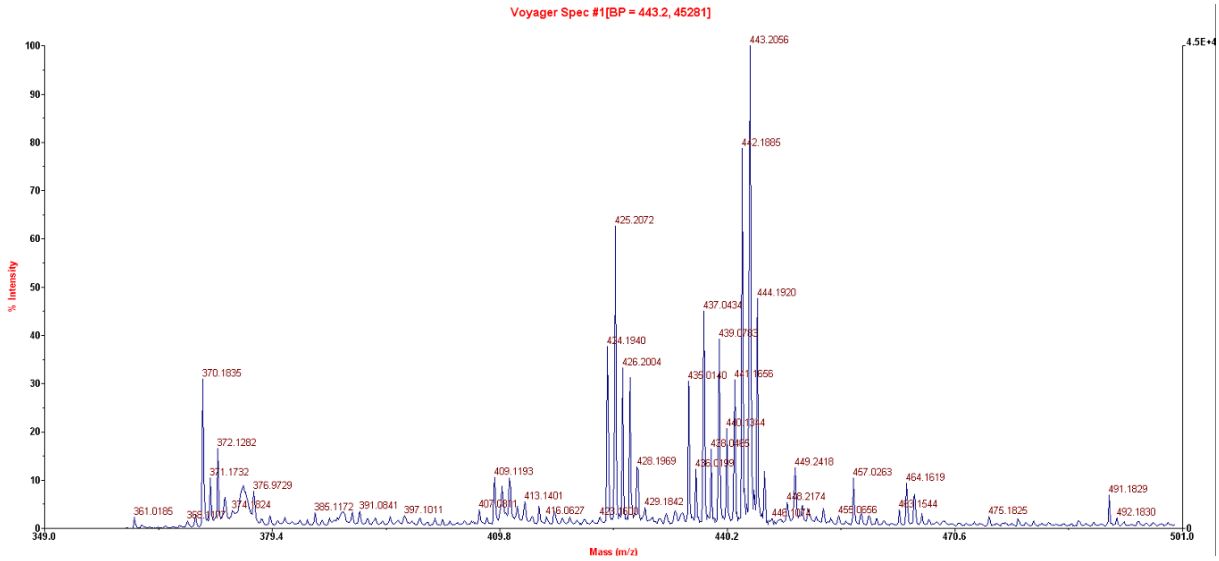

Figure S4. bTbK **2** - MALDI-TOF mass spectrum (dihydroxybenzoic matrix.)

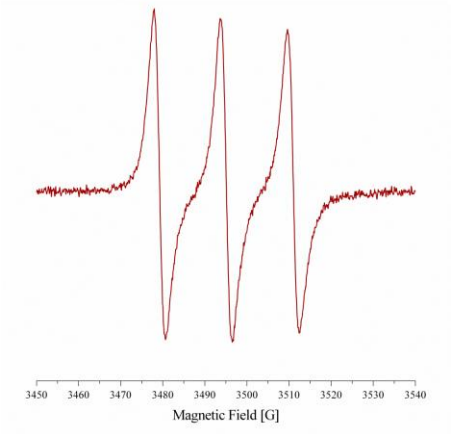

Figure S5. Solution EPR spectrum of bTbK **2** (100 µM in d_8-toluene) at room temperature at X-band microwave frequency (9.8 GHz.)

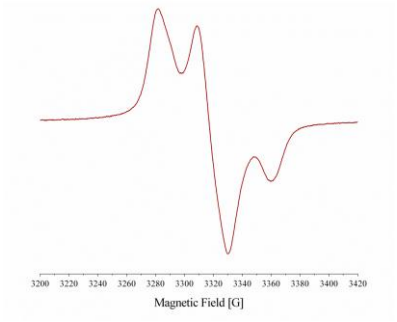

Figure S6. Frozen solution EPR spectrum of bTbK (100 μM in d_8-toluene) at 110 K at X-band microwave frequency (9.4 GHz.)

1-2. Synthesis of KCC-1-N

KCC-1 was synthesized using our reported protocol with a reaction time of 30 min.[1] Nitridation of KCC-1 was performed in a plug-flow fixed-bed quartz reactor by treating 0.5 g of KCC-1 with pure ammonia (300 mL/min) at various temperatures for 12 h. In the case of ^{15}N enriched samples, due to the cost and limited availability of ^{15}N-enriched ammonia gas, two quartz tube reactors were connected in series and 0.5 g of KCC-1 in each reactor was treated with ^{15}N-enriched (80%) ammonia gas (50 mL/min) for 3 h. Unreacted ammonia gas that came out of the 1st reactor (at 700°C) was used to treat KCC-1 in the 2nd reactor (at 1100°C).

2. NMR and EPR experiments

2-1. Experimental details

EPR experiments. EPR experiments were performed using X-band spectrometer operating at 9.81 GHz with respectively 100 kHz and 1G for modulation frequency and amplitude. The microwave power was set to 1 mW to avoid saturation. Spectra were acquired every minute after impregnation.

Sample preparation for solid-state DNP measurements. The samples were prepared at room temperature by impregnating nitridated KCC-1 samples with a 16 mM bTbK solution in TCE. The nitroxide biradical bTbK was chosen as polarizing agent since (i) nitroxide biradicals result in larger DNP signal enhancement than monoradicals with a lower concentration of unpaired electrons and (ii) bTbK is more soluble in organic solvents than TOTAPOL. Furthermore, the rigid tether of bTbK constrains the relative orientation of the two TEMPO moieties, so as to optimize the polarization transfer by cross-effect from electrons to protons. Nitridated KCC-1 materials are moisture-sensitive since water reacts with surface amine sites to form silanol groups. Hence, a non-aqueous solvent, TCE, was used for the impregnation and the samples were introduced under argon into a 3.2-mm sapphire rotor. Sapphire is nearly transparent to microwaves at 263 GHz.[2]

DNP-enhanced NMR experiments. The solid-state NMR experiments were performed at 9.4 T (400 MHz for ^1H) on a Bruker BioSpin Avance III DNP NMR spectrometer equipped with a triple resonance ^1H/X/Y 3.2-mm low-temperature (ca. 100 K) MAS probe (ν_r = 8 kHz) and a 263 GHz gyrotron.[3] The μw irradiation was transmitted through a corrugated waveguide. The microwave power delivered to the sample was approximately 6 W. The NMR spectra were acquired at a temperature of about 100 K, which was controlled by a Bruker BioSpin MAS cooling system.

The $^1H\rightarrow^{15}N$ and $^1H\rightarrow^{29}Si$ CPMAS spectra and the directly excited ^1H spectra were acquired with the microwave irradiation “on” and “off”. The ^1H 90° pulse duration was 2.5 μs and the CP contact time

was t_{CP} = 2 ms. During the CP transfer, the ^{1}H radiofrequency (rf) field was linearly ramped from 44 to 49 kHz, whereas the rf amplitude was constant and equal to 40 kHz for both ^{15}N and ^{29}Si. SPINAL64[4] proton decoupling was applied during the acquisition with a ^{1}H rf field amplitude of 95 kHz. Since the build-up time of the DNP-enhanced ^{1}H polarization is determined by $T_1(^1H)$, identical recovery delays were used in DNP-enhanced and conventional NMR experiments. To maximize the sensitivity, the recovery delay was chosen to be $1.3T_1(^1H)$.[5] The ^{15}N and ^{29}Si spectra of KCC-1 in natural isotopic abundance typically resulted from the accumulation of 8192 and 1024 scans, respectively, with a recovery delay of 11 s, leading to total experimental times of 25 h and 3 h. The ^{15}N spectra of ^{15}N-enriched KCC-1 were acquired using only 1024 scans in 3 h. The ^{1}H spectra resulted from the accumulation of 16 scans with a recovery delay of 11 s in a total time of 3 min. The ^{15}N isotropic chemical shifts were referenced to the NH_4^+ resonance of ammonium nitrate (δ_{iso} = 0 ppm) by using ^{15}N labeled proline dissolved in a 12 mM TOTAPOL solution in $^{2}H_2O/H_2O$/glycerol mixture as a secondary external chemical shift reference (δ_{iso} = 54.3 ppm). The chemical shifts given here may be converted to those relative to the common primary ^{15}N standard, nitromethane, by subtracting 358.4 ppm. The ^{29}Si chemical shifts are referenced to tetramethylsilane, using the ^{29}Si NMR signal of kaolinite as secondary reference.

Description of the fitting procedures. For the deconvolution of ^{29}Si and ^{15}N NMR spectra, each site was assumed to have a Gaussian lineshape due to the distribution of local geometries in amorphous materials. The fit of NMR signals was performed using dmfit and Matlab software.[6]

2-2. DNP-enhanced ^{1}H→^{15}N CPMAS spectra

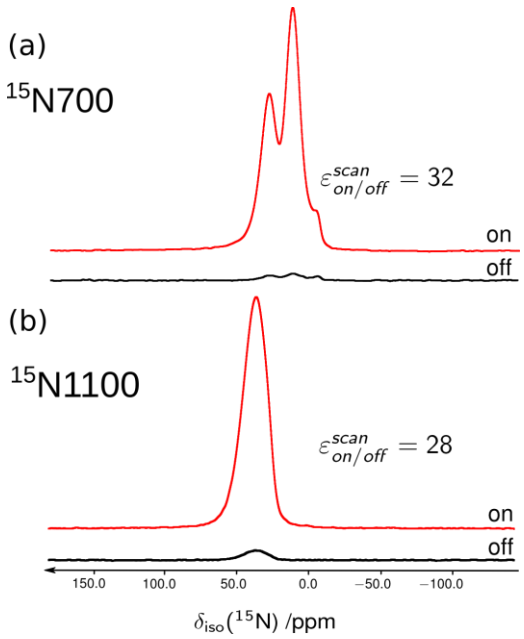

Figure S7. ^{1}H→^{15}N CPMAS spectra of (a) KCC-1-^{15}N700 and (b) KCC-1-^{15}N1100 samples impregnated with a 16 mM bTbK solution in TCE at 100 K, 9.4 T and ν_r = 8 kHz. The spectra with and without microwave irradiation are labeled "on" and "off". Additional experimental parameters are given in the section "Experimental details".

Time saving due to microwave irradiation for ^{1}H→^{15}N CPMAS spectra

The improvement in sensitivity between ^{1}H→^{15}N CPMAS experiments with and without microwave irradiation is characterized by the enhancement factor per unit of time[7]

$$\varepsilon_{on/off}^{time} = \frac{S_{on}N_{off}}{N_{on}S_{off}}\sqrt{\frac{T_{off}}{T_{on}}} \quad \text{(S1)}$$

where S_{on} , N_{on} and T_{on} are the signal intensity, the root-mean-square amplitude of the noise and the total acquisition time of ^{1}H→^{15}N CPMAS experiments with microwave irradiation, whereas S_{off} , N_{off} and T_{off} denote similar quantities for experiments acquired without microwave irradiation, all other experimental parameters being unchanged. We have recently shown that $\varepsilon_{on/off}^{time}$ factor can be expressed as[7]

$$\varepsilon_{on/off}^{time} = \varepsilon_{on/off}^{scan}\sqrt{\frac{T_1(^{1}\mathrm{H})}{T_{\mathrm{DNP}}(^{1}\mathrm{H})}} \quad \text{(S2)}$$

when the recycle delay of ^{1}H→^{15}N CPMAS experiments is chosen to be 1.3 times the build-up time constant of the ^{1}H polarization, so as to optimize the sensitivity.[5] Here, we found that $T_{\mathrm{DNP}}(^{1}\mathrm{H})$ = $T_1(^{1}\mathrm{H})$. Hence, according to Eq. S2, $\varepsilon_{on/off}^{time}$ is equal to $\varepsilon_{on/off}^{scan}$, which is about 30.

The acquisition time required to obtain a ^{1}H→^{15}N CPMAS spectrum without microwave irradiation with a signal-to-noise ratio S_{off}/N_{off} without microwave irradiation identical to S_{on}/N_{on} of the DNP-enhanced spectrum can be calculated by rewriting Eq. S1 as

$$T_{off} = \left(\varepsilon_{on/off}^{time}\frac{S_{off}N_{on}}{N_{off}S_{on}}\right)^2 T_{on} = \left(\varepsilon_{on/off}^{time}\right)^2 T_{on} \, . \quad \text{(S3)}$$

Here, T_{on} = 25 h and $\varepsilon_{on/off}^{time} \approx 30$. Hence, we have $T_{off} \approx 937$ days.

Table S1. Experimental ^{15}N NMR parameters extracted from the best-fit simulations of the DNP-enhanced $^{1}H \rightarrow ^{15}N$ CPMAS spectra shown in Fig. 2.

Sample	^{15}N environment	Integrated intensity /%	δ_{iso} /ppm	FWHM /ppm
KCC-1-N600	NH_2Si	39.1	9.5	9.5
	$NHSi_2$	60.9	25.1	13.9
KCC-1-^{15}N700	NH_4^+	5.7	−1.4	5.2
	NH_2Si	55.0	11.0	9.2
	$NHSi_2$	39.3	25.1	10.8
KCC-1-N800	NH_2Si	8.04	10.0	12.3
	$NHSi_2$	91.6	29.3	18.2
KCC-1-N900	NH_2Si	6.6	10.0	12.3
	$NHSi_2$	83.9	33.9	21.5
	NSi_3	9.5	55.0	18.6
KCC-1-^{15}N1100	$NHSi_2$	93.8	34.3	18.7
	NSi_3	6.2	55.0	18.6

2-3. DNP-enhanced ^{1}H MAS spectra

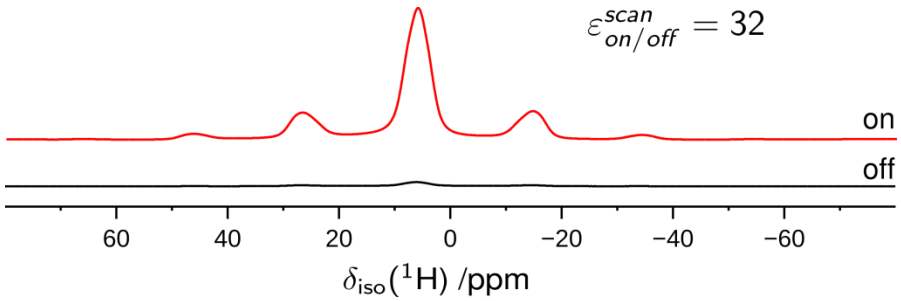

Figure S8. ^{1}H MAS spectra of KCC-1-^{15}N700 impregnated with a 16 mM bTbK solution in TCE at 100 K, 9.4 T and ν_r = 8 kHz. The spectra with and without microwave irradiation are labeled “on” and “off”. Additional experimental parameters are given in the section “Experimental details”.

2-4. DNP-enhanced ^{1}H→^{29}Si CPMAS spectra

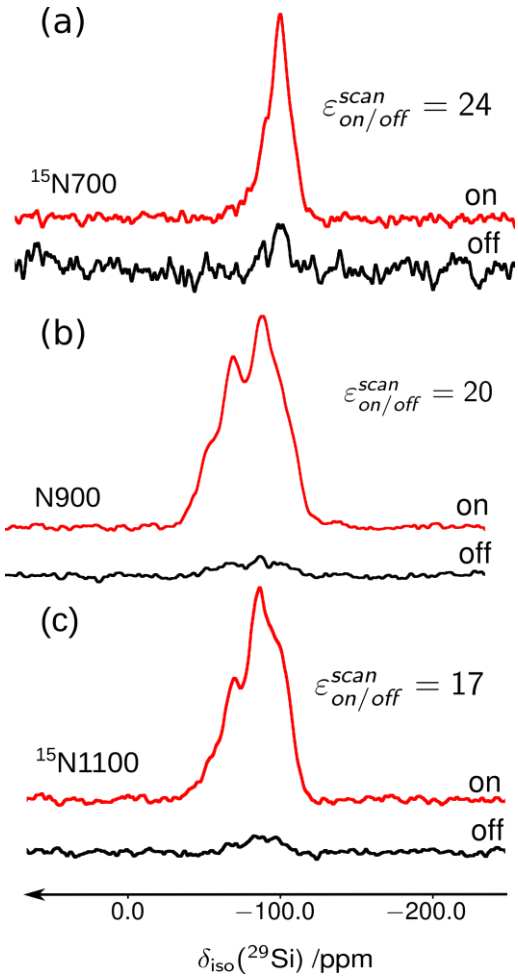

Figure S9. ^{1}H→^{29}Si CPMAS spectra of (a) KCC-1-^{15}N700, (b) KCC-1-N900 and (c) KCC-1-^{15}N1100 samples impregnated with a 16 mM bTbK solution in TCE at 100 K, 9.4 T and ν_r = 8 kHz. The spectra with and without microwave irradiation are labeled "on" and "off". Additional experimental parameters are given in the section "Experimental details".

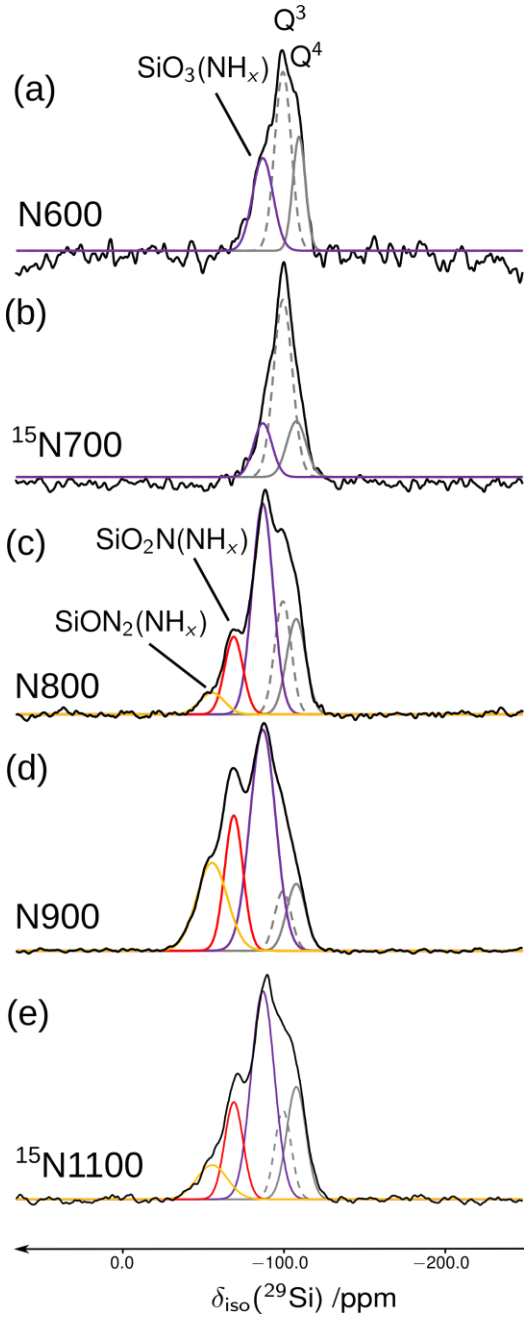

Figure S10. DNP-enhanced ^{1}H→^{29}Si CP-MAS spectra of (a) KCC-1-N600, (b) KCC-1-^{15}N700, (c) KCC-1-N800, (d) KCC-1-N900 and (e) KCC-1-^{15}N1100, all impregnated with a 16 mM bTbK solution in TCE at 9.4 T and ν_r = 8 kHz. The individual components of the best-fit simulations shown in orange ($SiON_2(NH)$), red ($SiO_2N(NH)$), purple ($SiO_3(NH)$), dashed grey (Q^3) and continuous grey (Q^4) lines using the parameters given in Table S2.

Fig. S9 shows how DNP can enhance the ^{1}H→^{29}Si CPMAS signals of KCC-1-N900 by a factor $\varepsilon_{on/off}^{scan} \approx 20$ with respect to conventional NMR at 100 K. Like for ^{15}N, we have $T_{DNP}(^{1}H) = T_1(^{1}H)$. Similar $\varepsilon_{on/off}^{scan}$ factors were measured for other KCC-1-N (Fig. S9). Note that the $\varepsilon_{on/off}^{scan}$ factors measured for ^{1}H→^{29}Si CPMAS spectra (see Fig. S9) are slightly lower than those measured for ^{1}H→^{15}N CPMAS spectra (see Fig. S7). Furthermore, the $T_{DNP}(^{1}H) = T_1(^{1}H)$ build-up time constants are about 11 s for ^{1}H→^{29}Si CPMAS spectra, instead of 8.5 s for ^{1}H→^{15}N CPMAS spectra. The reduction of $\varepsilon_{on/off}^{scan}$ factors and the lengthening of $T_{DNP}(^{1}H) = T_1(^{1}H)$ time

constants are believed to stem from the formation of crystalline domains of TCE, which leads to a phase separation between the solvent and the polarizing agent. In contrast to glycerol/water or DMSO/water mixtures. TCE is not a glass-forming solvent. Hence, thawing and freezing can alter the quality of the glass.[8]

The DNP-enhanced $^{1}H\rightarrow^{29}Si$ CPMAS spectra of KCC-1-N samples (Figs. S10) indicate that the structure of Si sites near the surface is affected by T_N. The ^{29}Si spectra of KCC-1-N600 and KCC-1-^{15}N700 are dominated by a peak near −100 ppm assigned to $Si(OSi)_3(OH)$ (Q^3) site.[9] These spectra also display peaks of $Si(OSi)_4$ (Q^4) and $SiO_3(NH_x)$ sites, at −108.3 and −87.5 ppm respectively.[10,11] For $T_N \geq 800$°C, the most intense peak stems from the $SiO_3(NH_x)$ sites with x = 1 or 2, although the spectra also display signals of Q^3 and Q^4 sites as well as of $SiO_2N(NH_x)$ and $SiON_2(NH_x)$ sites with x = 1 or 2 at −69.5 and −56.0 ppm respectively.[11] The $^{1}H\rightarrow^{29}Si$ CPMAS spectra of Fig. S10 differ from the previously reported ^{29}Si NMR spectra obtained by direct excitation without DNP[12] since the latter experiments show both bulk and surface sites, whereas CPMAS enhances signals of ^{29}Si sites near the surface.

Table S2. Experimental ^{29}Si NMR parameters extracted from the best fit simulations of DNP-enhanced $^{1}H\rightarrow^{29}Si$ CPMAS spectra shown in Fig. 3. Excellent fits of the experimental spectra were achieved by assuming only five distinct ^{29}Si environments: Q^4, Q^3, $SiO_3(NH_x)$, $SiO_2N(NH_x)$ and $SiON_2(NH_x)$, with x = 1 or 2. Nevertheless, other ^{29}Si sites, such as $Si(OSi)_2(OH)$ (Q^2), SiO_3N, SiO_2N_2 and $SiON_3$, should be present near the surface of KCC-1-N, but their signals are too weak to be detected, or may be masked by resonances of other sites.

Sample	^{29}Si environment	Integrated intensity /%	δ_{iso} /ppm	FWHM /ppm
KCC-1-N600	Q^4	39.3	−108.3	9.3
	Q^3	44.4	−100.0	12.0
	$SiO_3(NH_x)^a$	16.3	−87.5	15.3
KCC-1-^{15}N700	Q^4	19.9	−108.3	14.0
	Q^3	61.6	−100.0	13.6
	$SiO_3(NH_x)^a$	18.5	−87.5	13.5
KCC-1-N800	Q^4	18.2	−108.3	14.0
	Q^3	18.5	−100.0	12.0
	$SiO_3(NH_x)^a$	43.8	−87.5	15.3
	$SiO_2N(NH_x)^a$	14.2	−69.5	13.4
	$SiON_2(NH_x)^a$	5.3	−56.0	18.2
KCC-1-N900	Q^4	9.8	−108.3	14.0
	Q^3	7.5	−100.0	12.0
	$SiO_3(NH_x)^a$	43.2	−87.5	18.7
	$SiO_2N(NH_x)^a$	18.9	−69.5	13.4
	$SiON_2(NH_x)^a$	20.6	−56.0	22.4
KCC-1-^{15}N1100	Q^4	19.1	−108.3	14.0
	Q^3	12.9	−100.0	12.0
	$SiO_3(NH_x)^a$	42.9	−87.5	17.0
	$SiO_2N(NH_x)^a$	15.8	−69.5	13.4
	$SiON_2(NH_x)^a$	9.3	−56.0	22.4

[a] With x = 1 or 2.

3. Mechanism for the nitridation of KCC-1 nanoparticles

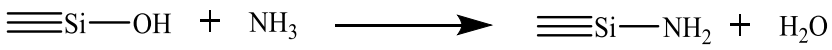

Scheme S3. The formation of a primary silylamine by the attack of ammonia on silanol group.

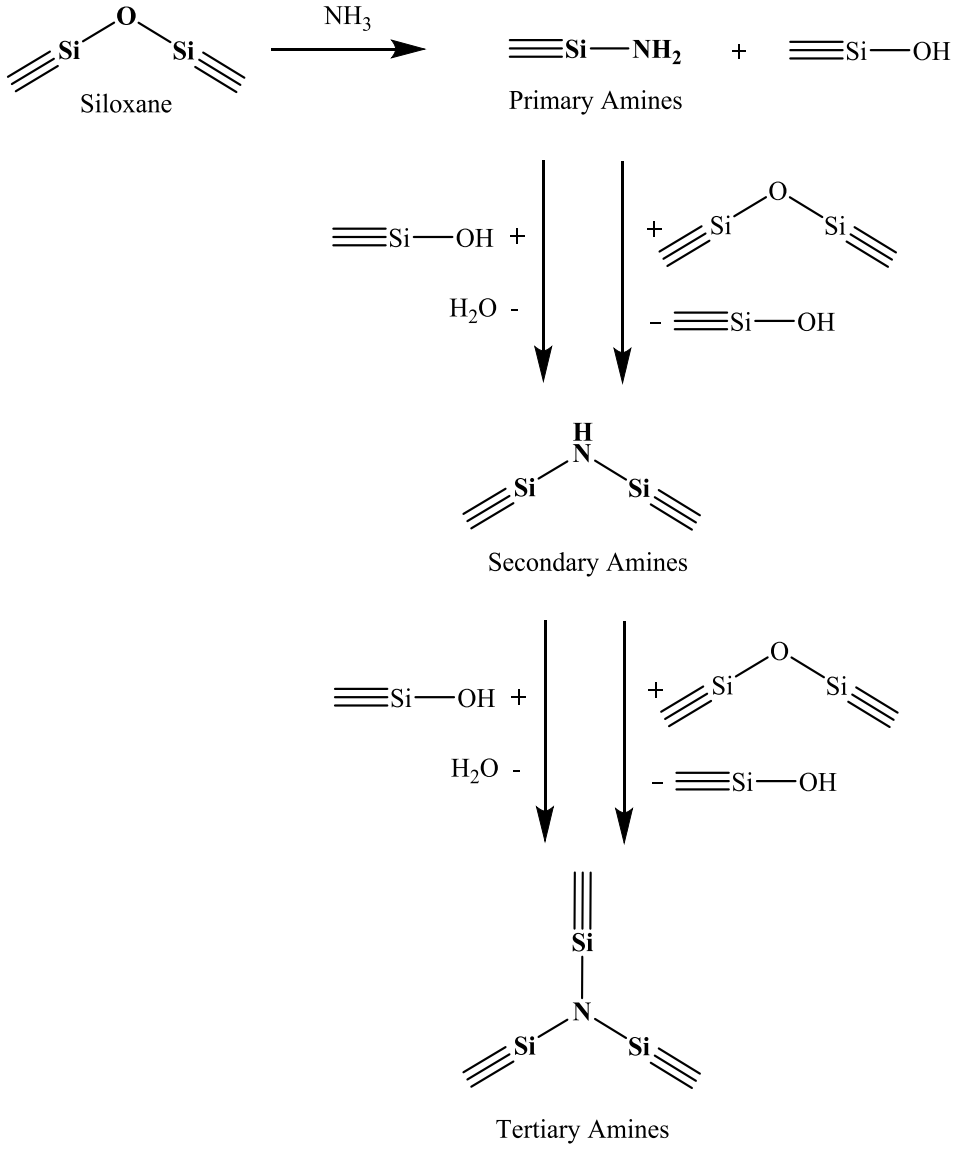

Scheme S4. The formation of primary silylamines by attack of ammonia on siloxane bridges and reaction schemes for the formation of secondary and tertiary amines.

The surface silanols react with ammonia, causing OH to be replaced by NH_2 (Scheme S3). These primary silylamine sites can also be formed by an attack of NH_3 on the siloxane (Si-O-Si) units of the silica framework to produce Si-NH_2 and additional silanols (1st step of Scheme S4). The ammonia can also be protonated by the acidic SiOH groups at the surface of KCC-1, forming ammonium ions observed for T_N = 700°C. The secondary silylamine $NHSi_2$ sites are formed by the attack of NH_2Si group on neighboring silanol groups and siloxane

bridges (2nd step of Scheme S4). Furthermore, the $NHSi_2$ site can attack neighboring silanol groups and siloxane bridges to form tertiary silylamine sites, NSi_3 (3rd step of scheme S4). Finally, $SiO_2N(NH_x)$ and $SiON_2(NH_x)$ sites are produced by reactions of NH_3 with siloxane bridges of SiO_3N and SiO_2N_2 moieties according to Scheme S4. The formation of $SiO_2N(NH_x)$ and $SiON_2(NH_x)$ groups explains why the nitrogen content increases with increasing T_N (see Table 1). If the only nitridation mechanism was the conversion of surface silanol groups into SiO_3NH_2 sites, the number of surface silanol groups in the starting KCC-1 material would limit the final nitrogen content. Here, we used the same starting material KCC-1 calcined at 550°C in air for all T_N, Hence the increase of the nitrogen content for higher T_N must result from the mechanism of Scheme S4.

References

[1] V. Polshettiwar, D. Cha, X. Zhang, J. M. Basset, *Angew. Chem. Int. Ed. Engl.* **2010**, *49*, 9652–9656.

[2] A. B. Barnes, G. De Paëpe, P. C. A. van der Wel, K.-N. Hu, C.-G. Joo, V. S. Bajaj, M. L. Mak-Jurkauskas, J. R. Sirigiri, J. Herzfeld, R. J. Temkin, et al., *Appl. Magn. Reson.* **2008**, *34*, 237–263.

[3] M. Rosay, L. Tometich, S. Pawsey, R. Bader, R. Schauwecker, M. Blank, P. M. Borchard, S. R. Cauffman, K. L. Felch, R. T. Weber, et al., *Phys. Chem. Chem. Phys.* **2010**, *12*, 5850–5860.

[4] B. M. Fung, A. K. Khitrin, K. Ermolaev, *J. Magn. Reson.* **2000**, *142*, 97–101.

[5] M. Pons, M. Feliz, E. Giralt, *J. Magn. Reson.* **1988**, *78*, 314–320.

[6] D. Massiot, F. Fayon, M. Capron, I. King, S. Le Calvé, B. Alonso, J.-O. Durand, B. Bujoli, Z. Gan, G. Hoatson, *Magn. Reson. Chem.* **2002**, *40*, 70–76.

[7] T. Kobayashi, O. Lafon, A. S. Lilly Thankamony, I. I. Slowing, K. Kandel, D. Carnevale, V. Vitzthum, H. Vezin, J.-P. Amoureux, G. Bodenhausen, et al., *Phys. Chem. Chem. Phys.* **2013**, *15*, 5553–5562.

[8] A. Zagdoun, G. Casano, O. Ouari, M. S. Der, A. J. Rossini, F. Aussenac, M. Yulikov, G. Jeschke, C. Cope, A. Lesage, et al., *J. Am. Chem. Soc.* **2013**, *135*, 12790–12797.

[9] O. Lafon, M. Rosay, F. Aussenac, X. Lu, J. Trébosc, O. Cristini, C. Kinowski, N. Touati, H. Vezin, J.-P. Amoureux, *Angew. Chem. Int. Ed.* **2011**, *50*, 8367–8370.

[10] T. Asefa, M. Kruk, N. Coombs, H. Grondey, M. J. MacLachlan, M. Jaroniec, G. A. Ozin, *J. Am. Chem. Soc.* **2003**, *125*, 11662–73.

[11] F. Hayashi, K. Ishizu, M. Iwamoto, *J. Am. Ceram. Soc.* **2010**, *93*, 104–110.

[12] M. Bouhrara, C. Ranga, A. Fihri, R. R. Shaikh, P. Sarawade, A.-H. Emwas, M. N. Hedhili, V. Polshettiwar, *ACS Sustain. Chem. Eng.* **2013**, *1*, 1192–1199.